WRIGHT, PETRA C., M.S. Cytotoxicity Screening Matrix Assisted Laser Desorption Ionization Mass Spectrometry for Nanoparticle Biomarker Detection. (2014)
Directed by Dr. N. H. Chiu. 54 pp.

Toxicology is a broad topic that aims to assess the risk of chemicals on living organisms. It has been acknowledged that everything is toxic to a living organism. What distinguishes a toxin from a remedy depends on the dose [1]. Presently, there are toxicity assays that are implemented for human risk assessment studies such as, 3-(4, 5-Dimethyl-2-thiazolyl)-2, 5-diphenyl-2H-tetrazolium bromide (MTT) assay and lactate dehydrogenase (LDH) assay; however, it has been shown that some toxins interfere with these assays. Carbon nanodots, an unknown toxicant has shown to interfere with the LDH assay. Therefore proper methods and techniques must be devised for the analysis of these unknown toxicants to enable the reliable risk assessment for humans.

In this study a new method was devised using, hydrogen peroxide and aflatoxin b1 as the known toxicants. The Cytotoxicity Screening Matrix Assisted Laser Desorption Ionization Time of Flight Mass Spectrometry (cs-MALDI-TOF-MS) technique was implemented as a viable approach to studying nanoparticle toxicity. Previously, Human liver (HepG2) cells were dosed with varying concentrations of these known toxicants and analyzed using cs-MALDI. In this study, Human monocyte (THP-1) cells were dosed with the same concentrations of these known toxicants as the HepG2 and analyzed. This study demonstrates that the two toxicants can be distinguished through the presence and absence of certain peaks using the cs-MALDI method. This method has been developed as a high throughput screening method that can lead to the future identification of biomarkers associated to each toxicant independently.

CYTOTOXICITY SCREENING MATRIX ASSISTED LASER DESORPTION IONIZATION MASS SPECTROMETRY FOR NANOPARTICLE BIOMARKER DETECTION

by

Petra C. Wright

A Thesis Submitted to
the Faculty of The Graduate School at
The University of North Carolina at Greensboro
in Partial Fulfillment
of the Requirements for the Degree
Master of Science

Greensboro
2014

Approved by

_____
Committee Chair

APPROVAL PAGE

This thesis has been approved by the following committee of the Faculty of The Graduate School at The University of North Carolina at Greensboro.

Committee Chair _____
Dr. N. H. Chiu

Committee Members _____
Dr. Nicholas Oberlies

_____
Dr. Mitchell Croatt

_____
Date of Acceptance by Committee

_____
Date of Final Oral Examination

TABLE OF CONTENTS

Page

LIST OF TABLES

Page

LIST OF FIGURES

Page

CHAPTER I

REVIEW OF LITERATURE

Toxicity Assays

Toxicology is the process of chemicals exerting toxic effects in biological systems [1]. There are many toxicity assays available that examine a specific mechanism such as oxidative stress, cell viability and cell death. These assays are utilized for risk assessment studies and are valuable methods for soluble chemicals. 2'7'-dichlorodihydrofluorescein is an assay that measures the formation of reactive oxygen species (ROS). This substrate penetrates cell membranes and gets hydrolyzed by cellular esterases. ROS converts the cleaved substrate to a fluorescent oxidation product. The amount of product detected correlates to the amount of ROS present. 3-(4, 5-dimethylthiazol-2-yl)-2, 5-diphenyltetrazoliumbromide (MTT) assay determines the cell viability by reducing the MTT salt to a purple MTT-formazan product. The amount of MTT-formazan present correlates to the metabolically active cells present. Lactate dehydrogenase (LDH) measures cellular necrosis by using a yellow tetrazolin salt (INT) as a substrate. When cell death occurs LDH is released from the cytosol and catalyzes the oxidation of INT to a red formazan product. The amount of INT detected correlates to cellular necrosis [24, 26].

These assays are limited to the evaluation of a single biomarker like LDH while the same toxicant may also have adverse effects on the other cellular activities. Thus, multiple different assays are often used to perform the risk assessment of new chemicals. Furthermore, for testing chemicals that may cause an unknown cytotoxicity, all the existing cell-based assays may need to be further developed to determine the unknown cytotoxicity.

Nanoparticles

Nanomaterials have emerged rapidly since the early 90's. They are small scale substances, usually <100 nm in size. Nanomaterials are engineered on the molecular level to achieve unique physical and chemical properties which make them useful in all types of environmental and medicinal products. These properties present new challenges to understanding the adverse effects of nanomaterials on human health [39]. Humans are exposed to different forms of nanomaterials throughout the lifetime of that nanomaterial [31]. The most common routes of exposure are ingestion, skin penetration, and inhalation [39]. It is of eminent concern for adequate testing to assess the human risk under real life situations. The current approaches to assess these risks are based on the classical toxicology methods. However, these methods cannot fully assess the risks due to the unique properties of the nanomaterials [31].

In the literature, nanoparticles are known to adsorb the reagents or dyes associated with these available assays thus skewing the assay results. Twenty four engineered nanoparticles that are well characterized were investigated for their possible interference with the classical toxicological assays. All 24 nanoparticles were found to interfere with at least one of the toxicological assays present [24]. Titanium dioxide (TiO_2) was one of the nanoparticles examined. It is an engineered nanoparticle that has the unique property of blocking UV light. This physical property has led to TiO_2 industrial use in sunscreens and water repellents. There are several forms of TiO_2 that exist and one of the most commonly studied is anatase. Anatase TiO_2 is a semiconductor that can generate reactive oxygen species which is detrimental to cells. In low concentrations, anatase TiO_2 is known to penetrate the skin [18, 39]. It has been observed that TiO_2 interferes with the detection of oxidation species, MTT and LDH assays at concentrations less than10 ug/mL. The limit of detection for these assays is 50 ug/mL [24]. In contrast, TiO_2 has shown

to have a high (100 ug/mL) and low (10 ug/mL) toxicity in THP-1 cell lines. Although the cell proliferation results indicated that both concentrations were toxic to THP-1 cells only the high concentration of 100 ug/mL was shown to have significant increases in LDH release [24, 37]. These results indicate that the classical toxicity assays used to test these nanomaterials are not consistent thus a new method is needed for accurately assessing toxicity. In this study, carbon nanodots were the nanomaterial readily available.

Carbon Nanodots

Carbon nanomaterials are present all around us. They are released upon incomplete combustion processes, inorganic dust from desert storms, candles and cigarettes. The most common route of exposure for carbon nanomaterials is inhalation. As with any nanomaterial, carbon based nanomaterials have many different forms of existence. Most of the carbon nanomaterials are known to induce cardiovascular toxicity and pulmonary toxicity patterns in humans. They can pass into the systemic circulation; induce inflammation in the lungs, fibrosis, and epithelioid granulomas. The ultrafine nanomaterials demonstrated increased pulmonary inflammation when compared to the fine-sized particulates. This indicates that there are more factors influencing toxicity other than particle size [26, 39].

Carbon nanodots are carbon based nanomaterials that are relatively new and are suspected to be non-toxic. They have good implication for bioimaging and have shown to be effective for cancer therapy [20, 21]. Carbon nanodots induce apoptosis in cancer cells, and are more effective against cancer in conjunction with UV radiation [19, 21]. Although these carbon nanodots are beneficial to the medicinal world, the toxicity is vastly unknown. Before these nanomaterials can be implicated in any type of treatment the risk assessment studies must be completed.

Matrix Assisted Laser Desorption Ionization Mass Spectrometry

Matrix Assisted Laser Desorption Ionization Mass Spectrometry (MALDI-MS) is a powerful source attached to a mass spectrometer that produces intact gas phase ions for large, non-volatile, thermally liable compounds such as proteins [2]. MALDI provides high throughput and high sensitivity analyses that can be readily automated. In comparison to other ionization methods, MALDI is non-destructive to large biomolecules and do not require chemical modifications [22].

In MALDI, the target analyte and matrix are co-crystallized onto the metal plate and a laser is fired onto the analyte/matrix crystals. The laser energy activates the matrix which vaporizes the analyte and they are both released into the gaseous phase. Once the transition to the gaseous phase occurs the sample is ionized by the matrix molecules. The matrix can accept and donate protons so the transfer of a proton can result in a positively charged sample ion or a negatively charged ion. Although MALDI is an efficient process there are still limitations associated with this method. It has a low efficiency to detect low mass ions due to the matrix ions generating strong signals usually below m/z 500. There is also a high molecular weight limitation where the sensitivity is lower due to the impact velocity of those high molecular weight ions. Another limitation is that the ionization of the sample can be suppressed when analyzing complex mixtures. Despite the limitations of MALDI, it has still proven to be one of the better techniques for protein analyses [22].

MALDI has been successful in identifying carcinoid tumor biomarkers and apoptotic biomarkers [13, 25]. It can distinguish mammalian cell lines and different strains of bacteria [5, 6, 30, 38]. MALDI has been used to detect the activation of macrophages and monitor viral proteins [15, 32]. Aside from proteomic studies, MALDI has also been applied to lipid profiling [7]. These varieties

of MALDI applications provide sufficient evidence to the diversity of the MALDI method. To this date, the MALDI method has not been used to detect toxicity of chemicals and particles. In this study, a MALDI method is devised for cytotoxicity studies of nanomaterials. MALDI seems to be the most viable approach to nanomaterial toxicity since there aren't any reagents or products for interference. Nanomaterials such as carbon nanodots and titanium dioxide have been used as matrices for MALDI applications to address the limitations of the MALDI method [12, 29, 35]. Therefore it is known that these nanomaterials won't interfere with the MALDI method, they are in fact compatible.

CHAPTER II

INTRODUCTION

Statement of Problem

Toxicology is a broad topic that aims to assess the risk of chemicals on living organisms. Presently, there are toxicity assays that are implemented for human risk assessment studies such as, 3-(4, 5-Dimethyl-2-thiazolyl)-2, 5-diphenyl-2H-tetrazolium bromide (MTT) assay and lactate dehydrogenase (LDH) assay; however, it has been shown that some toxins interfere with these assays. Furthermore, since the current assays evaluate a single biomarker multiple assays are used for risk assessment studies. This represents both time and financial burden for many toxicological studies, even for the bigger companies in the pharmaceutical industry. Our goal was to further develop a method known as Cytotoxicity Screening Matrix Assisted Laser Desorption Ionization Time of Flight Mass Spectrometry (cs-MALDI-TOF-MS) to perform screening for cytotoxicity.

Hypothesis

With the ability to detect multiple peptides and/or proteins simultaneously in a single MALDI-TOF MS measurement, we hypothesize that there is sufficient resolving power from using MALDI-TOF MS measurements to distinguish various cellular responses that result from the exposure of a specific cell line to different toxic chemicals.

Specific Aim 1

Our first aim was to identify an approach to determine the cytotoxicity of carbon nanodots, an unknown toxicant. Simultaneously, we attempted to define the toxicity of the carbon nanodots utilizing the conventional lactate dehydrogenase (LDH) assay and cell counting method.

Specific Aim 2

The second aim was to establish a high throughput screening method to differentiate a mammalian cell line exposed to different toxicants using cs-MALDI-TOF-MS.

CHAPTER III

CYTOTOXICITY OF CARBON NANODOTS

Introduction

Carbon nanomaterial production has increased globally in the past few years and risk assessment for carbon nanomaterials is not completely understood [39]. Their physical and chemical properties allow them to be great candidates for imaging, photocatalysis, cancer cell inhibition, and disease diagnosis [6, 19, 21, 36]. Although carbon nanodots (CD) are considered to be biocompatible, there have been cases where CD is identified as toxic agent for various biological tissues [6, 19]. Therefore, it is important that the risk assessment is thoroughly examined before administering them for medicinal use. The correlation between exposure to nanoparticles and vascular diseases is of particular concern [3]. Monocytes are known to play a crucial role in development of inflammable vascular diseases and have been suggested to be significant targets for nanoparticle exposure [4].

Currently, various toxicity assays that are used for known toxins have been applied to nanomaterials where the toxicity is unknown [24]. Lactate dehydrogenase (LDH) assay has been considered a gold standard for measuring cytotoxicity. This common enzyme is shared amongst all cells and is released upon damage to the cell membrane. The LDH assay had been used to access the toxicity of CD, as support to CD inducing apoptosis versus necrosis [19]. The toxicity of CD was assessed utilizing the LDH assay and the cell counting method. This study investigates the possible interference of the carbon nanodots on the LDH assay in human monocyte THP-1 cells.

Materials and Methods

All reagents were of HPLC grade and obtained from Sigma-Aldrich.

Carbon Nanodots

Carbon nanodots used in this study were synthesized by Dr. Martin Choi and his research group in the Department of Chemistry at the University of Hong Kong Baptist University in Hong Kong, China. The CD has an approximate molecular weight of 2500-3200 g/mol and is approximately 2.2-5.0 nm in size. The CD's are comprised of a carbon core with amine, amide and carboxylic acid moieties covering its surfaces (Figure 1).

Figure 1. Carbon Nanodot

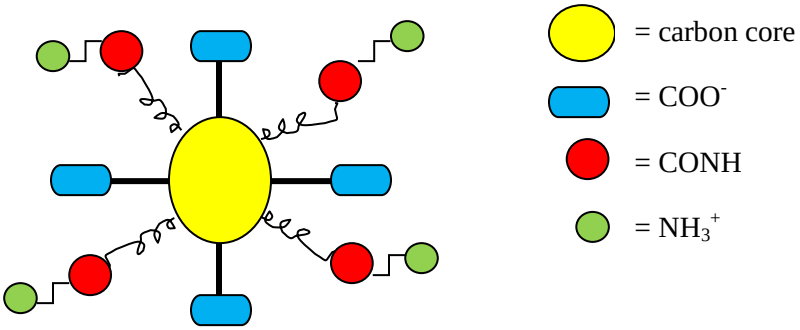

Carbon Nanodot comprised of carbon core, carboxylic acid, amine and amide moieties.

Cell Culture and Treatment

The human monocyte (THP-1) cells (ATCC, Manassas, VA) were maintained in RPMI-1640 medium supplemented with 10 % fetal bovine serum, 1 % penicillin-streptomycin antibiotic in 5 % CO_2 at 37 $^{\circ}$C. Prior to confluence, the cells were collected and centrifuge at 4 $^{\circ}$C, 1000 g for 10 min. The supernatant was decanted and the cell pellet was re-suspended in 10 mL Dulbecco's Modified Eagles Medium (DMEM). The cells were seeded in a 24-well plate at a density of $4.0x10^5$ cells per well. CD (0.60 mg) were mixed with 1 mL DMEM, an aliquot (400 uL) of this mixture was added to each well, which was incubated for 24 h.

LDH Assay

The cytotoxic effects of CD were first measured by quantitating the release of lactate dehydrogenase (LDH) from the THP-1 cells. Following incubation, an aliquot (200 uL per well) of treated cells were centrifuged at 4 $^{\circ}$C, 3.4 rpm for 5 min. The untreated cells (200 uL per well) were sonicated then centrifuged. The supernatants were collected for LDH measurements. Reagents for LDH assay were added 60 uL of 0.8 mg/mL pyruvate, 60 uL of 3 mg/mL NADH. The PBS (1 X, pH 7.4) volume varied according to sample volume. NADH was added last, for a total volume of 600 uL, to start the reaction and the cuvette was immediately placed in the spectrophotometer. In the spectrophotometer, the LDH reaction (Figure 2) is related to the oxidation of the NADH compound which absorbs at 340 nm, the reduced NAD does not absorb at this wavelength. The absorbance was recorded over 5 min.

Figure 2. LDH Reaction

$$H^+ + \text{pyruvate} + \text{NADH} \longrightarrow \text{L-lactate} + NAD^+$$

Trypan Blue Viability Assay

The cell number and cell viability were determined using cell counting method. Cells (100 uL per well) were mixed with trypan blue dye (100 uL) and 20 uL of this cell dye mixture was loaded onto a hemacytometer. For this study, each well was counted four times using both chambers of the hemacytometer. An aliquot (10 uL) of the cell dye mixture was added onto a microscope slide and observed using an EVOS® digital microscope.

Measurement of CD interference with LDH

The CD (0.15 mg/mL) was dissolved in diH_2O (0.25 mL) for absorbance measurements. Serial dilutions were performed for concentrations of 0.45, 0.30, 0.15, 0.075 mg/mL. The CD solution (10 uL) was added to the LDH reagents 60 uL NADH, 60 uL pyruvate, 490 uL 1X PBS, and absorbance was read at 340 nm.

Results and Discussion

The lactate dehydrogenase (LDH) assay is widely used to detect cytotoxicity of various nanoparticles. In this study, the cytotoxicity of monocytes, after exposure to CD in concentrations ranging from 0.075 to 0.60 mg/mL, was determined by using the LDH assay. Figure 3 displays the LDH absorbance in the presence and absence of CD. There was a pronounced effect of LDH release in the cell lysate (Figure 3, positive control) indicating LDH was utilizing NADH in its conversion to pyruvate. The decrease in NADH absorbance over time confirmed that the reagents and instrument were operating properly. However, after 24 h incubation with 0.15 mg/mL and 0.30 mg/mL of CD, the CD did not cause an increase in the release of LDH in the THP-1 cells and the 0.30 mg/mL treatment was higher than the 0.15 mg/mL treatment (Figure 3).

Figure 3. Carbon Nanodot Toxicity using LDH assay

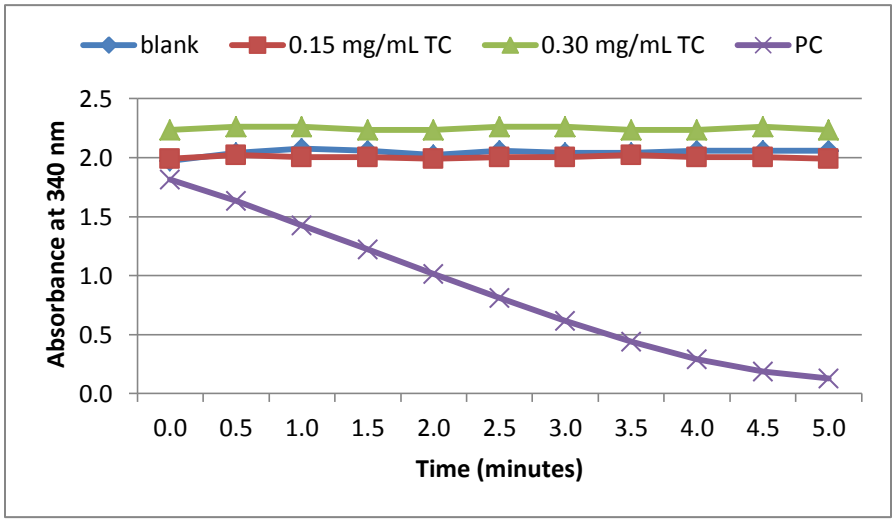

Carbon Nanodot toxicity using LDH assay. Blank contains 1 X PBS, positive control (PC) contains supernatant from lysed THP-1 cells, and treatment (TC) contains 0.15 and 0.30 mg/mL of carbon nanodots respectively.

To validate the results of LDH assay, the cell count method with trypan blue staining was used. This method was optimized by counting the chambers of a hemacytometer four times for each cell culture of THP-1 cells. The living and dead cells were both counted and averaged to get the total number of cells (Figure 4). Incubation of cells with various concentrations of CD for 24 h caused a significant decrease in cell viability measured by trypan blue staining (Figure 5). The cell morphology changes by CD were further examined with a digital microscope (Figure 6). Compared to control, the cells treated with CD display significant changes in cell morphology including a loss of uniformity and detritus surrounding the cell clusters as indicated by the arrows in Figure 6. The inconsistency results between Figure 3 (LDH assay) and Figures 5-6 (trypan blue staining and digital microscope) by CD treatment lead us to propose that the CD was interfering with the NADH absorbance of the LDH assay in Figure 3.

Figure 4. Cell Counting Accuracy

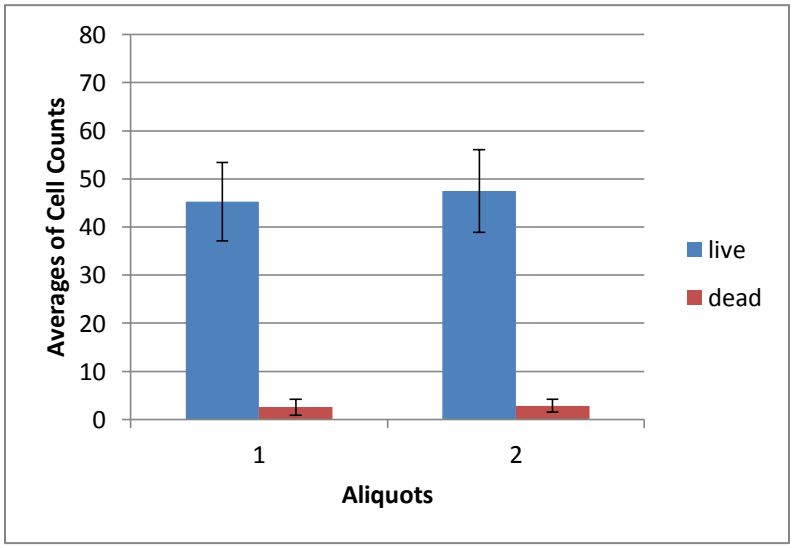

Cell Counting Accuracy determined by cell counting with trypan blue staining and hemacytometer. Live cells and dead cells were counted and averaged (n=4). The values are mean ± standard deviation.

Figure 5. Carbon Nanodot Toxicity using Cell Counting Method

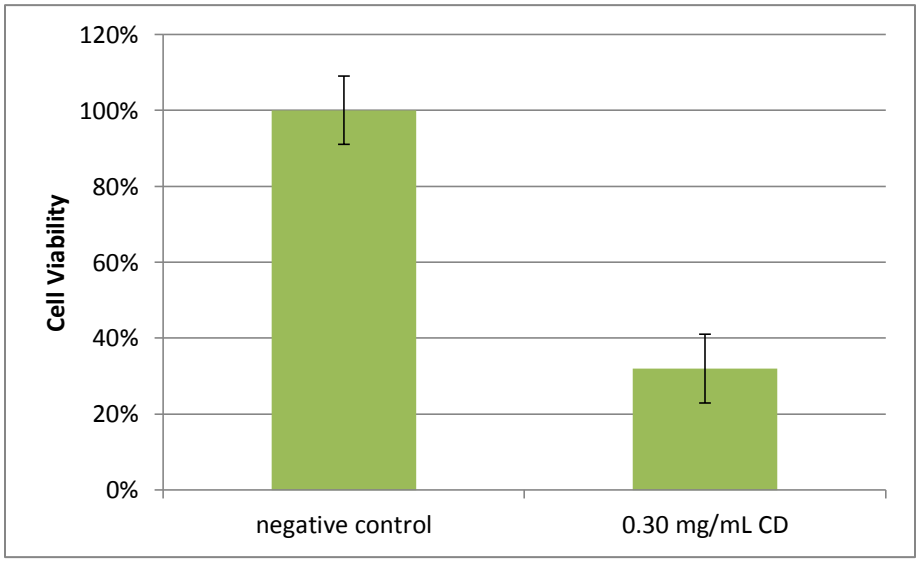

Carbon Nanodot Toxicity determined by trypan blue staining and hemacytometer. The percentage of viable cells from 0.30 mg/mL CD treatment was normalized to negative control. The reported values are mean ± standard deviation with n=4 and $p < 0.05$.

Figure 6. THP-1 Cell Death Morphology

A) CD treated **B) Control**

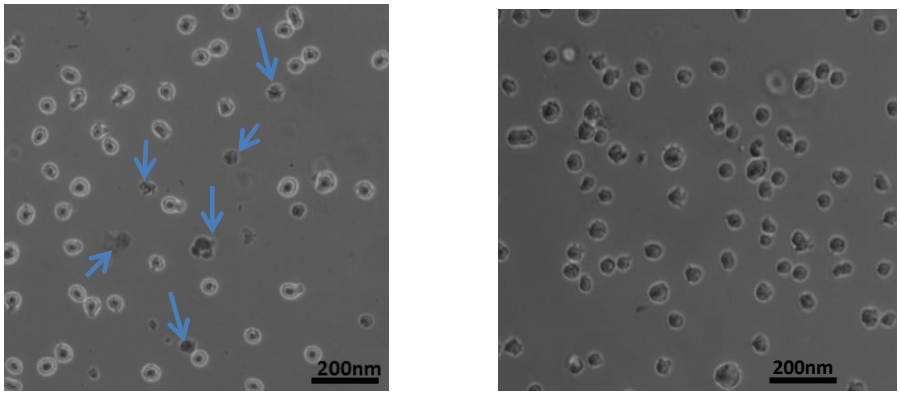

THP-1 Cell Death Morphology. A) Presence of cellular debris and loss of uniformity for THP-1 cells exposed to CD, indicated by the blue arrows. B) THP-1 cells under normal cell culture conditions, cells appear to maintain their uniformity.

The absorbance of CD at 340 nm was measured to further study the interference with the LDH assay (Figure 7). The absorbance of CD in the absence of THP-1 cells was measured in concentrations ranging from 0.075 to 0.60 mg/mL. The absorbance of the CD at 340 nm increased as the concentrations increased (R^2= .9883, Figure 7). This trend was observed in the LDH measurement, suggesting that there was interference on the NADH absorbance (340 nm) by the CD.

Figure 7. CD Absorbance at 340 nm

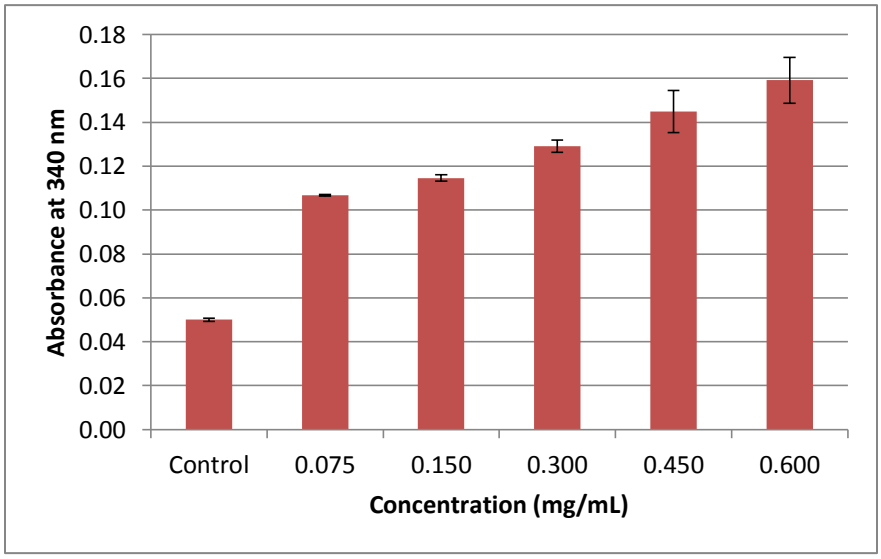

CD absorbance at 340 nm. Control contains 1 X PBS. The reported values are mean ± standard deviation, n=3 with $p < 0.05$.

In this study, we are the first to report that the CD was found to interfere with the NADH absorbance of the LDH assay at 340 nm in a dose-dependent manner supporting our speculation that CD interferes with the LDH assay. Our results suggest that the lactate dehydrogenase assay should not be used to evaluate the cytotoxicity of CD that potentially leads to a false conclusion on the cytotoxicity of carbon nanodots as reported in the literature. The traditional trypan blue staining method proved to be a viable approach for evaluating the cytotoxicity of nanomaterials, whose chemical and physical properties may not be known. This method has been used to access the cytotoxicity of multi-walled carbon nanotubes, however, it is fairly time consuming. Therefore, an improved method is needed to determine the risk assessment of CD for future use.

CHAPTER IV

CYTOTOXICITY SCREENING MATRIX ASSISTED LASER DESORPTION IONIZATION MASS SPECTROMETRY

Introduction

Matrix assisted laser desorption ionization mass spectrometry (MALDI-MS) has been applied extensively to the proteomic field [15, 23]. This technique has been used to define biomarkers specific to apoptotic cell death, to differentiate primary blood cells, and to study activation of macrophages [8, 23]. To the best of our knowledge, as MALDI-MS applications tend to diversify, it has yet to be used to examine cytotoxicity in mammalian cells. In this study, we evaluate MALDI-MS as a new methodology to examine cytotoxicity (cs-MALDI-MS).

The sample preparation is critical for successful cs-MALDI-MS analysis. In generating cs-MALDI mass spectra from the human monocyte (THP-1) cell line, there are many experimental factors that can influence the quality of mass spectra produced. For optimum cs-MALDI-MS analyses of THP-1 cells each parameter of our protocol was optimized. The work flow consists of harvesting the cells, washing the cells, and mixing the cells with matrix for direct analysis.

Materials and Methods

All of the reagents used were of HPLC grade and purchased from Sigma-Aldrich.

Cell Culture and treatment

The cell culture harvest method, see Chapter III. After harvesting the cells, the supernatant was decanted and the cell pellet was re-suspended in RPMI-1640 for a density of $1.0x10^7$ cells per mL. The cells were seeded in a 6-well plate and treatments were added to the proper wells, which was incubated for 24 h. Aflatoxin b1 (10 mg) was dissolved in DMSO (.8 mL), it was administered to THP-1 cells in 100 uM and 400 uM concentrations. Hydrogen peroxide (9.5 M, 1mL) was diluted in 1 X PBS (9 mL) and was administered in 100 uM and 500 uM concentrations.

Trypan Blue Viability Assay

The cell viability was determined using cell counting method. Cells (10 uL) per well were mixed with trypan blue dye (90 uL) and 20 uL of this cell dye mixture was loaded onto a hemacytometer. Each well was counted four times using all four grids of the hemacytometer chamber.

cs-MALDI sample preparation

The THP-1 cells (~1 mL) were collected from each well and centrifuged at 4 $^{\circ}$C, 3.4 rpm for 10 min. The supernatant was decanted and the cell pellet was re-suspended in 1 mL PBS (1 X, pH 7.4). The cells were centrifuged at 4 $^{\circ}$C, 3.4 rpm for 10 min, for the completion of one wash. This was repeated two times with 1 X PBS (1 mL) and two times with 150 mM ammonium acetate (1 mL). THP-1 cell pellet was re-suspended in 150 mM ammonium acetate with a final concentration around 10^7 cells per microliter. The matrix, α-CHCA (10 mg) was dissolved in 1 mL of 50 % acetonitrile and 0.1 % trifluoracetic acid. Serial dilutions with α-CHCA and THP-1 cells were performed with a final cell concentration of 120,000 per uL. One microliter of

cell/matrix solution was spotted onto MALDI plate, and the solvent was evaporated at room temperature.

cs-MALDI analysis

cs-MALDI-MS mass spectra of THP-1 cells were obtained using a Waters Synapt G2 HDMS Optics MALDI-MS. A pulsed nitrogen laser (337 nm) was used for desorption/ ionization and mass spectra were acquired in positive linear mode. The instrument was operated with an acceleration potential of 25 kV. The quad profile was set to favor the low mass and the external mass calibration was performed using insulin and ATCH fragment from the Proteo-Mass Peptide and Protein MALDI-MS Calibration Kit. Spectra were obtained by accumulating data collected from 80 scans with 0.5 sec scan time.

Results and Discussion

1. Effect of Washing

The THP-1 cell growth reached ~90% confluence at 3 days and were harvested for treatment. Although cs-MALDI-MS is known to produce good quality spectra in the presence of salts, the presence of serum in the supplemented growth media can interfere with the spectral interpretation. Therefore, prior purification of the cell culture is needed to improve the quality of the mass spectra. To remove cellular debris, the cell culture must undergo several numbers of washing steps, three washes with 1X PBS (pH 7.4) and two washes with 150 mM ammonium acetate. To minimize the osmosis process during each washing step, which may lead to the cellular disruption, the use of different washing solutions were evaluated. In order to simulate the washing process, 1 mL of cells were collected and re-suspended in 1 mL solution for a time period of 30 minutes. The cellular integrity was evaluated every 5 min by comparing the cells in

solutions with the cells that were kept under the normal cell culturing conditions. The ammonium acetate and 1 X PBS solutions provided the best conditions for the time period.

During the washing process, the cells were counted after each washing step to determine the amount of loss (Figure 8). This step was critical to ensuring there was enough sample for cs-MALDI analysis. Before seeding the cells into the incubation plate, the cell loss was subtracted, approximately 20 % for 1 X PBS and approximately 65 % for ammonium acetate.

Figure 8. Effect of Washes on Cell Concentration

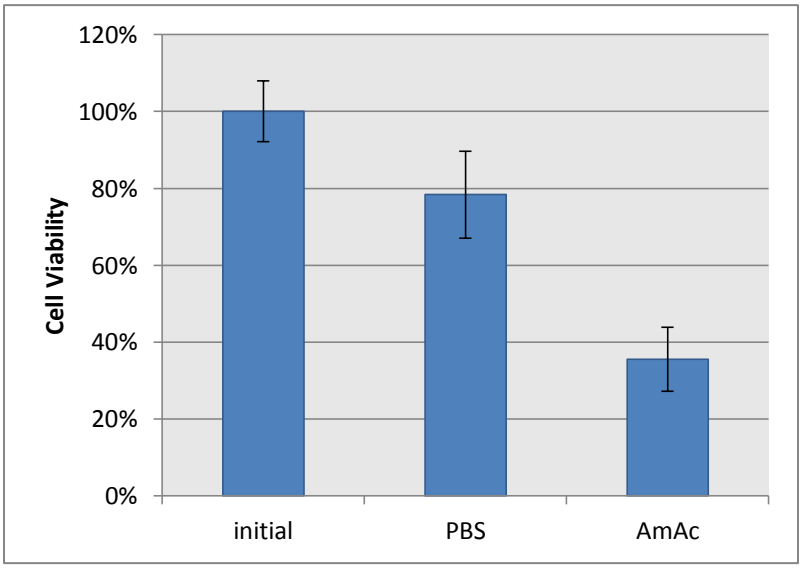

Effect of Washes on Cell Concentration. An initial cell count was performed before washing steps were performed. Cells were counted after each washing step and normalized the percentage of viable cells were normalized to the initial cell count. The reported values are mean ± standard deviation, n=4.

2. Effect of Cell Concentration

The cellular sample in this study is co-crystallized with the matrix and spotted onto the MALDI plate. For MALDI analysis it is necessary to have the proper ratio of matrix to target analyte(s). The number of matrix molecules should exceed the number of target analyte(s) such that the target analyte(s) don't cluster together, which would decrease desorption/ionization efficiency during the MALDI process. On the other hand, there must be enough number of target molecules in the MALDI sample. To ensure having the optimal ratio of matrix to intact cells, different number of cells were used ranging from 10^3 to 10^9 cells per spot were examined for cs-MALDI analysis (Figure 9). The results indicated that to achieve the highest signal with the lowest signal to noise ratio, 120,000 cells per spot was the best for this cell line. Any cell number higher than 120,000 cells per spot interfered with the desorption process.

Figure 9. Effect of Cell Concentrations on cs-MALDI Spectra

A) 1 million, 100 thousand, and 10 thousand cells per spot

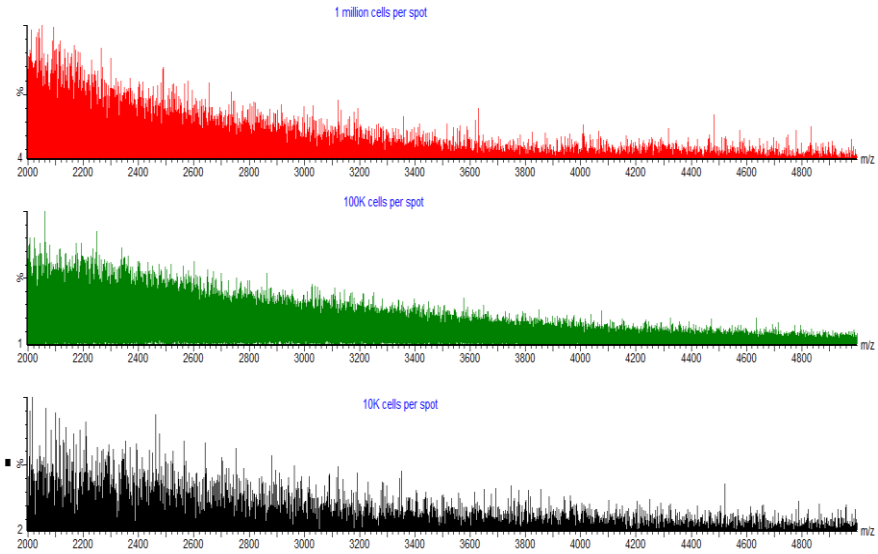

B) 120 thousand cells per spot

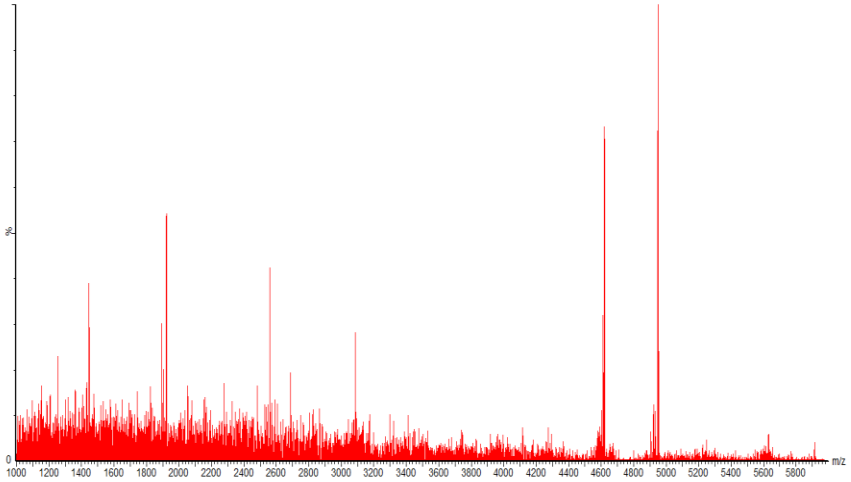

3. Effect of Different Matrices that have been used for measuring cellular samples

Selecting the appropriate matrix for optimum cs-MALDI analyses is an important issue. The matrix is used to minimize the damage inflicted by the laser on the cells. This ensures that the cellular integrity is not compromised and that the change in protein expression is caused by the exposure to the toxin and not the infliction from the laser. The matrix increases the energy of transfer from the laser to the cells thus increasing the sensitivity. 4-hydroxy-α-cyanocinnamic acid (α-CHCA) and sinapinic acid (SA) have both been reported in the literature as good matrices for large biomolecules. Both α-CHCA and SA were tested with the protein/peptide standards from a Proteo-Mass Peptide and Protein MALDI-MS Calibration Kit (Sigma Aldrich), and the spectrum for SA contained sodium adducts. Therefore the best matrix for our studies that produced a clean spectrum was the α-CHCA.

4. cs-MALDI analysis

The samples were analyzed with a Waters Synapt G2 HDMS Optics MALDI-MS. The MALDI-MS instrumental parameters were varied in their settings to favor low mass and high mass (Table 1). These parameters were selected based on our own experience as well as the recommendation from the manufacturer. Emphasis was put on optimizing the efficiency on transmitting various ions through the quadrupole at the front end of the instrument. However, the high mass settings wouldn't produce a good, consistent signal without high background noise, and lower signals were obtained when the peaks were detected above 7 kDa (Figure 10). After many attempts we shifted to the low mass settings with the quad profile favoring a mass range of 1 kDa to 6 kDa. These settings provided the better quality spectra for cs-MALDI analysis (Figure 9b). Although we tried adjusting many of the instrumental parameters using the peptide/protein standards to favor the high mass, the ionization efficiencies varied and the detection was low.

This could be attributed to larger proteins having lower ionization efficiencies or that the smaller proteins and peptides are more abundant.

Table 1. cs-MALDI-MS Settings

	Low Mass 1-6 kDa	**High Mass 2-12 kDa**
Source		
Sample Plate	10.0 kV	20.0 kV
Hexapole	15.0 kV	5.0 kV
Auto Values		
Detector	2925	2925
RF Settings		
Trap	350	320
IMS TOF	350	380
Transfer	350	380
Hexapole	550	600
TriWave		
Source Wave Height	Disabled	1.0 V
Transfer Wave Height	Disabled	3.0 V
Collision Energy		
Trap CE	Disabled	40.0
Transfer CE	Disabled	10.0
Trap DC		
Bias	Disabled	22
IMS DC		
Entrance	Disabled	2
Quad Profile		
Mass 1 (dwell time) [ramp time]	1000 (2) [95]	1000 (2) [95]
Mass 2 (dwell time)	6000 (2)	8000 (2)
Mass 3	6000	8000

Figure 10. High Mass cs-MALDI Spectrum

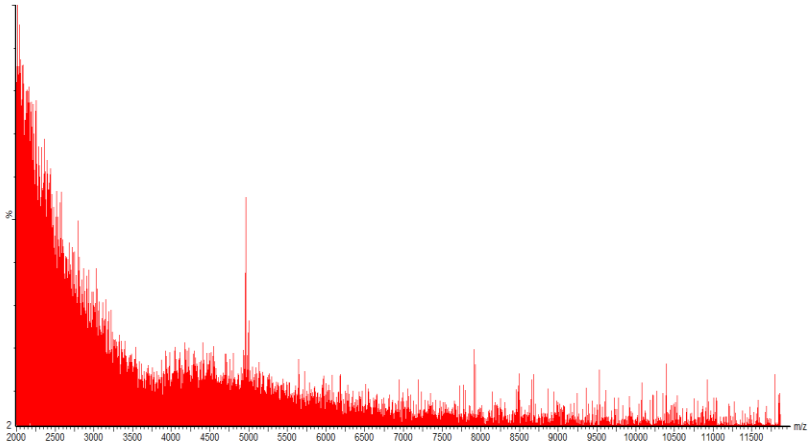

cs-MALDI Spectrum obtained from 10,000 THP-1 cells with no prior treatment using High Mass settings in Table 1.

5. cs-MALDI Analysis of Different Toxic Chemicals

MALDI-MS is widely used in distinguishing cell lines. In this study, a method for direct, cMALDI-MS was established and evaluated. To optimize the cMALDI direct analysis of THP-1 cells suspended in matrix, the cells were treated with hydrogen peroxide and analyzed. Hydrogen peroxide is a reactive oxygen species (ROS) that can generate more toxic ROS and induce oxidative stress in most cell types [1]. Hydrogen peroxide was administered to THP-1 cells in 100 uM and 500 uM concentrations and analyzed using cs-MALDI-MS and the standard trypan blue staining method. The cell viability was determined post exposure (Figure 11) confirming cellular death had occurred after 24 h incubation. Replicate experiments were performed from three independent cell cultures, and the same peak pattern is obtained each time (Figure 12). The cs-MALDI method developed in this study demonstrates the possibility to distinguish the variations in protein expression by simply comparing the differences in the spectral patterns which can be obtained directly from untreated and treated cells.

Figure 11. Hydrogen Peroxide Cell Viability

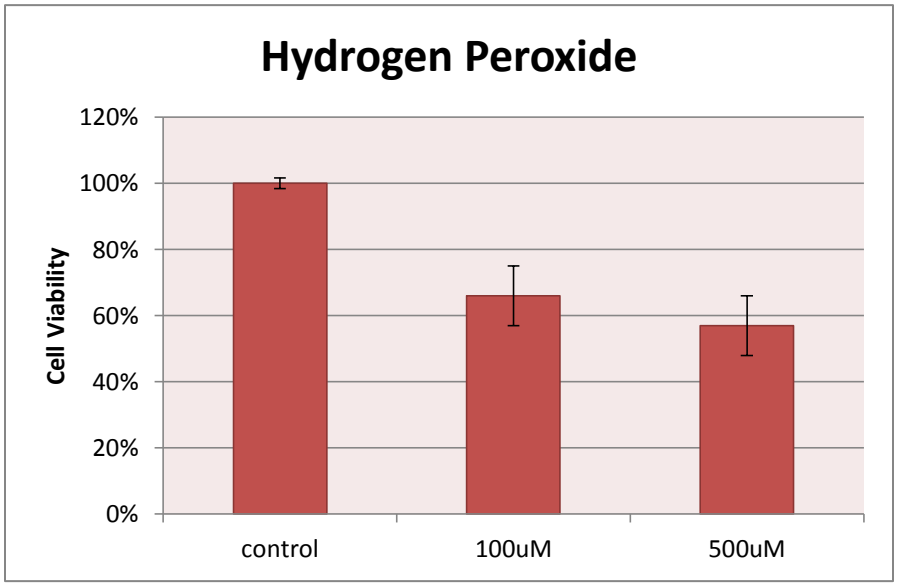

Cell Viability determined using trypan blue staining and hemacytometer. Cell count was performed post 24 h exposure to hydrogen peroxide. The percentage of viable cells post exposure was normalized to the control. The values are mean ± standard deviation, n=4.

Figure 12. cs-MALDI-MS for Hydrogen Peroxide

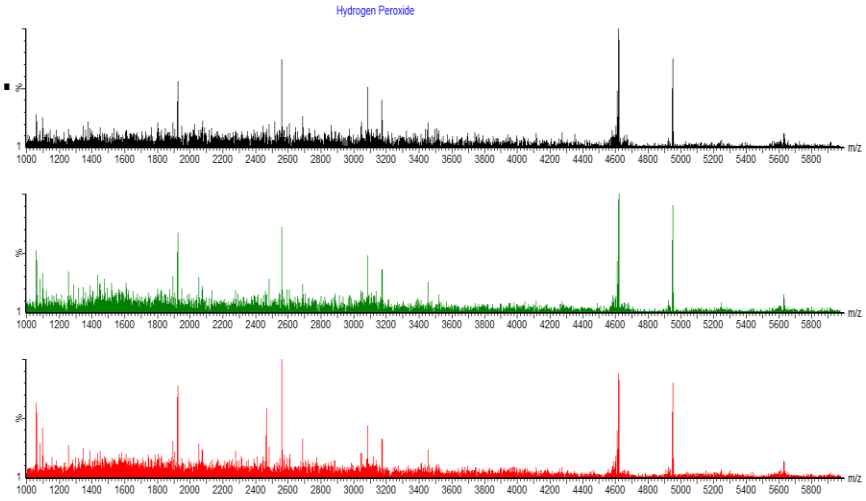

cs-MALDI spectra post 24 h incubation with hydrogen peroxide. Replicates were performed from different cell cultures, n=3. Spectra were obtained in positive linear mode using low mass settings.

To demonstrate the applicability of the cs-MALDI-MS method, THP-1 cells were treated with aflatoxin b1 from the *Aspergillus* species. Aflatoxin B1 is commonly found in food products such as nuts and corn. It is the most toxic metabolite in the aflatoxin family and is known to affect the liver [25]. In this study, aflatoxin b1 was administered to the THP-1 cells in concentration of 100 uM and 400 uM. The cell viability was determined post exposure (Figure 13) indicating cellular death had occurred after 24 h incubation. The mass spectra obtained from cs-MALDI-MS analysis of aflatoxin exhibited a number of discrete peaks in the m/z range that were different from the hydrogen peroxide mass spectra.

To confirm the differences in mass spectra, THP-1 cells were analyzed using cs-MALDI-MS with no prior treatment. These results indicated that THP-1 cells treated with aflatoxin and hydrogen peroxide will produce a unique mass spectral pattern (Figure 14). As shown in Figure 14, profiles for aflatoxin b1 and hydrogen peroxide are easily distinguished by visual inspection and the spectral patterns are reproducible. While many of the major peaks observed for all conditions are common, there are also a number of unique peaks (Figure 14, solid red arrow) and missing peaks (Figure 14, dotted red arrow). Visual inspection is enhanced by the zooming in on specific regions of the mass spectra to better identify peaks (Figure 15). Table 2 summarizes these common peaks, the peaks specific to each condition and the relative intensities observed during cs-MALDI-MS analysis. Principal component analysis was performed using the peaks summarized in Table 2. The results indicated that although there is little overlap in the spectral pattern of aflatoxin b1 and hydrogen peroxide, they can be separated into three segments (Figure 16). The blue dots in Figure 16 correspond to the peaks and the circles correspond to the group of peaks for each toxicant. This pattern can be used to distinguish which toxin is responsible for initiating a particular cellular response and is beneficial for screening purposes.

Figure 13. Aflatoxin B1 Cell Viability

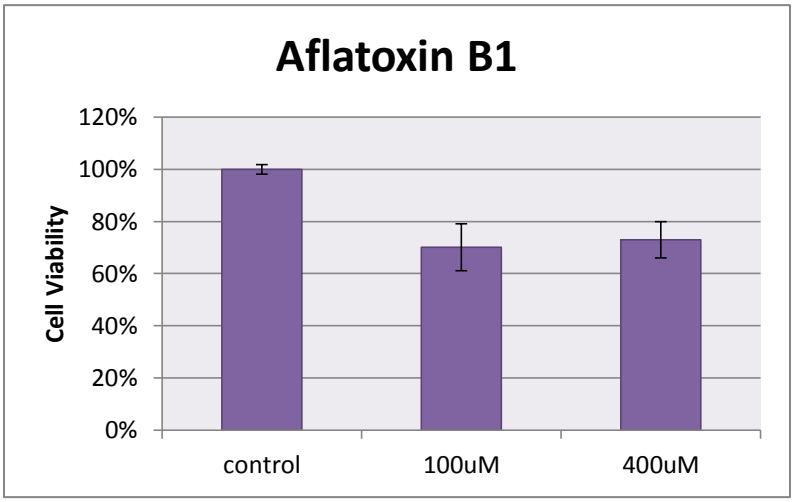

Cell Viability determined using trypan blue staining and hemacytometer. Cell count was performed post 24 h exposure to aflatoxin b1. The percentage of viable cells post exposure was normalized to the control. The values are mean ± standard deviation, n=4.

Figure 14. cs-MALDI-MS

A) Case #1

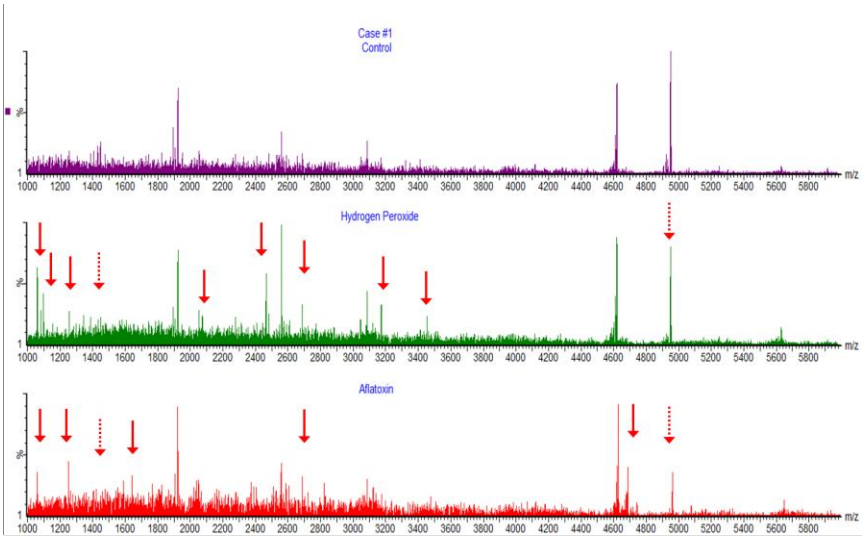

Key:

= new peaks

= missing peaks

B) Case #2: Replication of Case #1

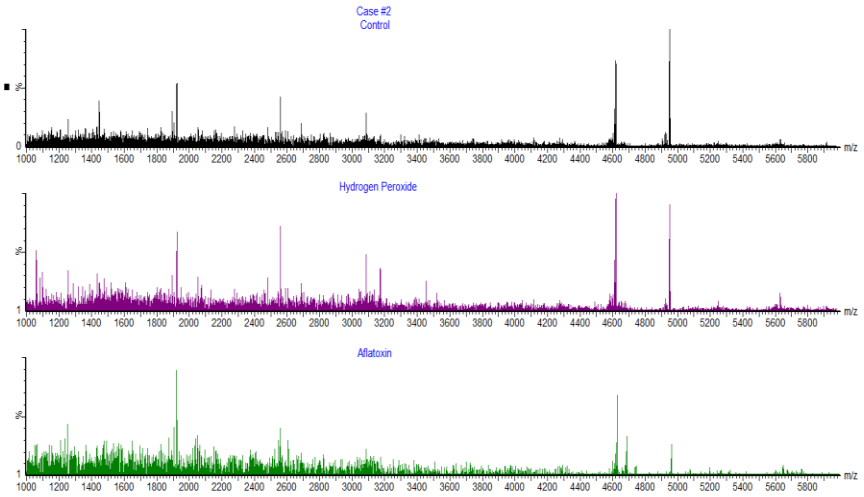

Figure 15. cs-MALDI-MS Expanded View

A) Zoom in view of 1 kDa- 3 kDa

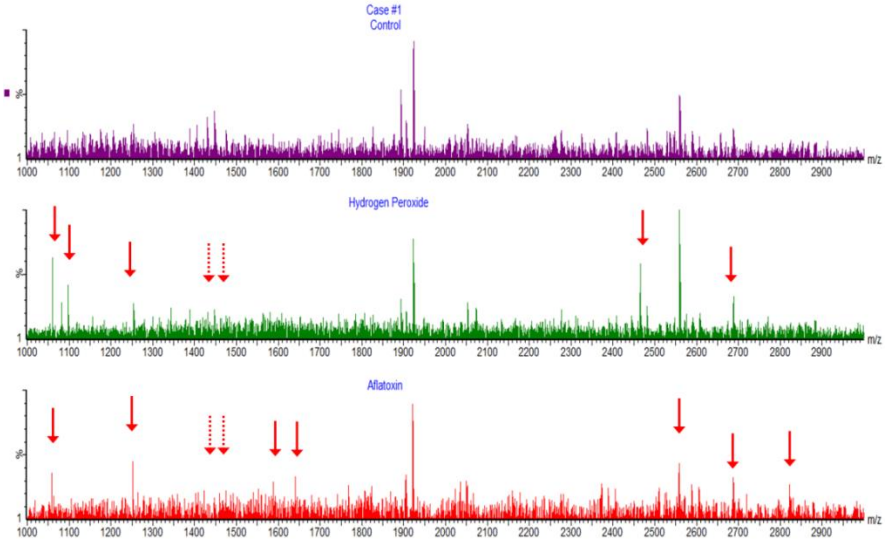

B) Replication of A

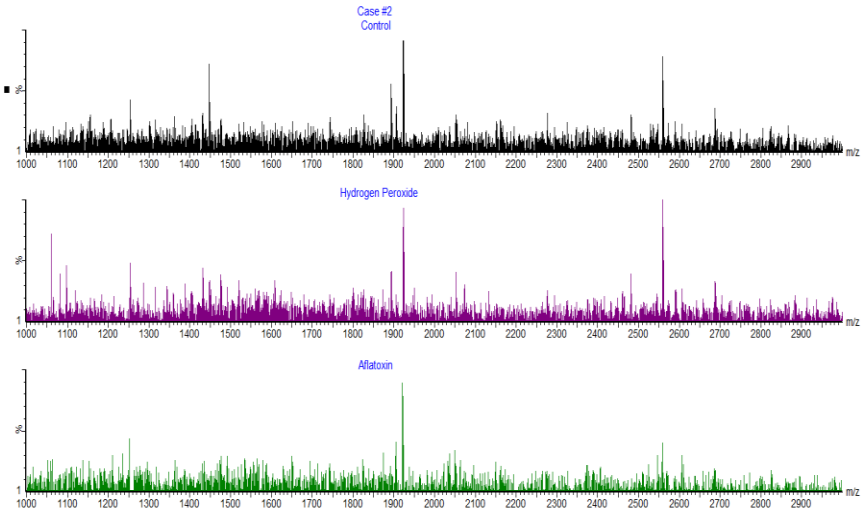

C) Zoom in view of 3000 Da - 3560 Da

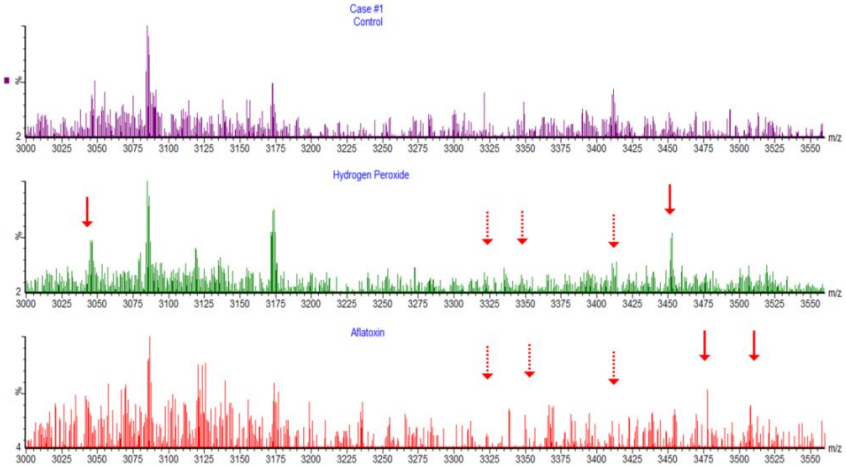

D) Replication of C

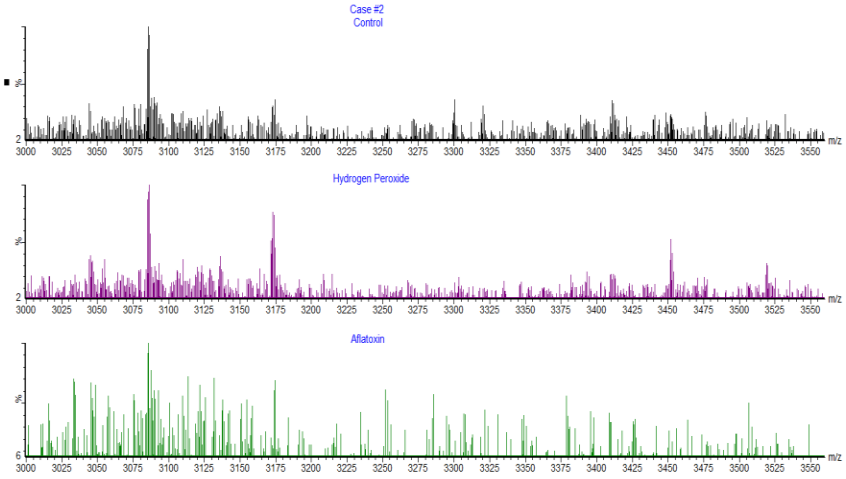

Table 2. List of cs-MALDI Peaks

Key: √ = peak present
- = peak not present
√- = peak intensity decreased compared to control
√+ = peak intensity increased compared to control
() = (intensity)

Peaks (m/z)	Untreated	H_2O_2	Aflatoxin B1
1058	- (0)	√ (70)	√- (40)
1096	- (0)	√ (35)	- (0)
1404	√ (30)	- (0)	- (0)
1447	√ (20)	- (0)	- (0)
1587	- (0)	- (0)	√ (30)
1640	- (0)	- (0)	√ (40)
1923	√ (70)	√ (90)	√ (100)
2510	- (0)	√ (70)	- (0)
2559	√ (30)	√ (20)	√ (40)
2687	- (0)	- (0)	√ (30)
2822	- (0)	- (0)	√ (30)
3321	√ (10)	- (0)	- (0)
3349	√ (10)	- (0)	- (0)
3411	√ (10)	- (0)	- (0)
3454	- (0)	√ (20)	- (0)
3477	- (0)	- (0)	√ (20)
3507	- (0)	- (0)	√ (15)
4620	√ (75)	√+ (100)	√+ (90)
4686	- (0)	√ (30)	√ (40)
4950	√ (100)	√- (30)	√- (37)

Figure 16. PCA of Common Peaks

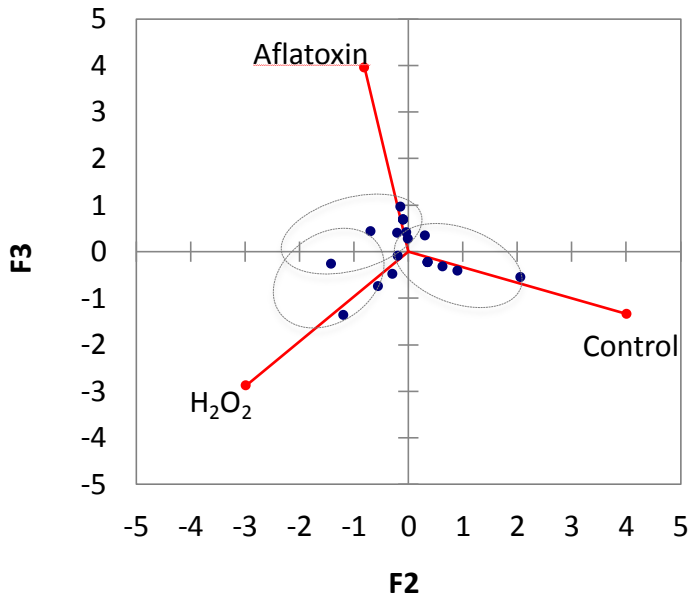

Principal Component Analysis of common peaks. Blue dots represent peaks from Table 2. Circles represent peaks associated with toxic chemical in quadrants.

The specific peaks for each condition can be utilized as a "fingerprint." It is important to note that further identification of the protein/peptide peaks can be accomplished by using the standard proteomic method, and may lead to the discovery of novel biomarkers that correspond to aflatoxin or hydrogen peroxide treatment with THP-1 cells or equivalence. The cs-MALDI method has been applied using HepG2 cells and the same toxic chemicals, differences in mass spectral patterns were observed there as well. This is the first time a MALDI method has been used to distinguish the cellular responses resulted from exposure to known toxic chemicals. These results provide sufficient support for using the cs-MALDI methodology in other toxicology studies including the nanoparticle toxicity studies

CHAPTER V

CONCLUSIONS AND FUTURE WORK

Conclusion

This study successfully demonstrated a novel application of cs-MALDI-MS for the detection of cytotoxicity. As shown, the cs-MALDI mass spectra of untreated, aflatoxin b1 and hydrogen peroxide were significantly different. These results provided significant evidence that the mass spectra of carbon nanodots can be different with some peaks in common, assuming CD cause different type of stress to THP-1. This method requires minimal sample preparation and volume, and avoids the use of reagents or dyes that is known to interfere with nanoparticles. The analytical process can be completed within 5 min. after sample preparation and can be readily automated for high-throughput analysis.

Significance of Study

Nanoparticle toxicity is of particular concern. Humans are exposed to carbon based nanomaterials daily and they have been found to induce cardiovascular toxicity. Although their unique properties have advantages in cancer therapy, their adverse effects are unknown. Carbon nanodots have been shown to interfere with the toxicological assay, lactate dehydrogenase, eliminating its use for toxicity studies. To the best our knowledge, there aren't any current assays that can accurately assess the risk of nanoparticles without interference. Information obtained from cs-MALDI-MS can be used to characterize nanoparticle effects on human health whether it's adverse or advantageous. The identification of biomarkers can increase the efficacy of treatment and monitoring of nanoparticle toxicity.

Future Work

In the future, it would be beneficial to administer carbon nanodots as treatment in a dose dependent manner and analyze with cs-MALDI-MS. THP-1 cells were studied in this work, and previously HepG2 cells, however they are not the only cell lines that can be affected by carbon nanodots. It is interesting to further study the effect of carbon nanodots on other cancer cell lines. Quantitation work of the biomarkers is important and can be easily achieved using dose-dependent treatments. Quantitation results can give insight to the complexity of cs-MALDI-MS method and provide useful information about the extent of damage due to nanoparticle toxicity. Such work would optimize cs-MALDI-MS as a universal screening method for chemicals and particles.

REFERENCES

1. Boelsterli, U. A. *Mechanistic toxicology: the molecular basis of how chemicals disrupt biological targets*; CRC Press, 2007.
2. Hoffmann, E. *Mass spectrometry*; Wiley Online Library, 1996.
3. Mossman, B. T.; Borm, P. J.; Castranova, V.; Costa, D. L.; Donaldson, K.; Kleeberger, S. R. *Particle and Fibre Toxicology* **2007**, *4*, 4.
4. Prach, M.; Stone, V.; Proudfoot, L. *Toxicology and Applied Pharmacology* **2013**, *266*, 19–26.
5. Vargha, M.; Takáts, Z.; Konopka, A.; Nakatsu, C. H. *Journal of microbiological methods* **2006**, *66*, 399–409.
6. Zhang, X.; He, X.; Li, Y.; Zhang, Z.; Ma, Y.; Li, F.; Liu, J. *Journal of Nanoscience and Nanotechnology* **2013**, *13*, 5254–5259.
7. Zhang, Y.; Li, H.; Ma, Y.; Lin, J. *Science China Chemistry* **2013**, 1–5.
8. Ahlf, D. R.; Compton, P. D.; Tran, J. C.; Early, B. P.; Thomas, P. M.; Kelleher, N. L. *Journal of Proteome Research* **2012**, *11*, 4308–4314.
9. Bergquist, J. *Chromatographia* **1999**, *49*, S41–S48.
10. Berhanu, D.; Dybowska, A.; Misra, S. K.; Stanley, C. J.; Ruenraroengsak, P.; Boccaccini, A. R.; Tetley, T. D.; Luoma, S. N.; Plant, J. A.; Valsami-Jones, E. *Environmental Health* **2009**, *8*, S3.
11. Bourdon, J. A.; Saber, A. T.; Jacobsen, N. R.; Williams, A.; Vogel, U.; Wallin, H.; Halappanavar, S.; Yauk, C. L. *Cardiovascular Toxicology* **2013**, *13*, 406–412.

12. Chen, S.; Zheng, H.; Wang, J.; Hou, J.; He, Q.; Liu, H.; Xiong, C.; Kong, X.; Nie, Z. *Analytical Chemistry* **2013**, *85*, 6646–6652.
13. Dong, H.; Shen, W.; Cheung, M. T. W.; Liang, Y.; Cheung, H. Y.; Allmaier, G.; Kin-Chung Au, O.; Lam, Y. W. *The Analyst* **2011**, *136*, 5181.
14. Foucaud, L.; Goulaouic, S.; Bennasroune, A.; Laval-Gilly, P.; Brown, D.; Stone, V.; Falla, J. *Toxicology in Vitro* **2010**, *24*, 1512–1520.
15. Franco, C. F.; Mellado, M. C. M.; Alves, P. M.; Coelho, A. V. *Talanta* **2010**, *80*, 1561–1568.
16. Ge, G.; Wu, H.; Xiong, F.; Zhang, Y.; Guo, Z.; Bian, Z.; Xu, J.; Gu, C.; Gu, N.; Chen, X. *Nanoscale research letters* **2013**, *8*, 1–10.
17. Hanrieder, J.; Wicher, G.; Bergquist, J.; Andersson, M.; Fex-Svenningsen, Å. *Analytical and Bioanalytical Chemistry* **2011**, *401*, 135–147.
18. Horie, M.; Kato, H.; Fujita, K.; Endoh, S.; Iwahashi, H. *Chemical Research in Toxicology* **2012**, *25*, 605–619.
19. Hsu, P.-C.; Chen, P.-C.; Ou, C.-M.; Chang, H.-Y.; Chang, H.-T. *Journal of Materials Chemistry B* **2013**, *1*, 1774.
20. Hu, Q.; Paau, M. C.; Zhang, Y.; Chan, W.; Gong, X.; Zhang, L.; Choi, M. M. F. *Journal of Chromatography A* **2013**, *1304*, 234–240.
21. Juzenas, P.; Kleinauskas, A.; George Luo, P.; Sun, Y.-P. *Applied Physics Letters* **2013**, *103*, 063701.
22. Kafka, A. P.; Kleffmann, T.; Rades, T.; McDowell, A. *International Journal of Pharmaceutics* **2011**, *417*, 70–82.
23. Khlebtsov, N.; Dykman, L. *Chemical Society Reviews* **2011**, *40*, 1647.

24. Kroll, A.; Pillukat, M. H.; Hahn, D.; Schnekenburger, J. *Archives of Toxicology* **2012**, *86*, 1123–1136.

25. Kuo, T.-R.; Chen, J.-S.; Chiu, Y.-C.; Tsai, C.-Y.; Hu, C.-C.; Chen, C.-C. *Analytica Chimica Acta* **2011**, *699*, 81–86.

26. Landsiedel, R.; Ma-Hock, L.; Kroll, A.; Hahn, D.; Schnekenburger, J.; Wiench, K.; Wohlleben, W. *Advanced Materials* **2010**, *22*, 2601–2627.

27. Lee, C. H.; Rajendran, R.; Jeong, M.-S.; Ko, H. Y.; Joo, J. Y.; Cho, S.; Chang, Y. W.; Kim, S. *Chemical Communications* **2013**, *49*, 6543.

28. Leong, Y.-H.; Rosma, A.; Latiff, A. A.; Ahmad, N. I. *Mycotoxin Research* **2011**, *27*, 207–214.

29. Ma, Y.; Zhang, X.; Zeng, T.; Cao, D.; Zhou, Z.; Li, W.; Niu, H.; Cai, Y. *ACS Applied Materials & Interfaces* **2013**, *5*, 1024–1030.

30. Munteanu, B.; Reitzenstein, C.; Hänsch, G. M.; Meyer, B.; Hopf, C. *Analytical and Bioanalytical Chemistry* **2012**, *404*, 2277–2286.

31. Oomen, A. G.; Bos, P. M. J.; Fernandes, T. F.; Hund-Rinke, K.; Boraschi, D.; Byrne, H. J.; Aschberger, K.; Gottardo, S.; von der Kammer, F.; Kühnel, D.; Hristozov, D.; Marcomini, A.; Migliore, L.; Scott-Fordsmand, J.; Wick, P.; Landsiedel, R. *Nanotoxicology* **2013**, 1–15.

32. Ouedraogo, R.; Daumas, A.; Ghigo, E.; Capo, C.; Mege, J.-L.; Textoris, J. *Journal of Proteomics* **2012**, *75*, 5523–5532.

33. Park, J.; Park, J.-H.; Ock, K.-S.; Ganbold, E.-O.; Song, N. W.; Cho, K.; Lee, S. Y.; Joo, S.-W. *Journal of Colloid and Interface Science* **2011**, *363*, 105–113.

34. Reddy, A. R. N.; Narsimha Reddy, Y.; Rama Krishna, D.; Himabindu, V. *Toxicological & Environmental Chemistry* **2010**, *92*, 1697–1703.

35. Shen, Q.; Dong, W.; Yang, M.; Baibado, J. T.; Wang, Y.; Alqouqa, I.; Cheung, H.-Y. *Food Research International* **2013**, *54*, 2054–2061.

36. Tang, J.; Kong, B.; Wu, H.; Xu, M.; Wang, Y.; Wang, Y.; Zhao, D.; Zheng, G. *Advanced Materials* **2013**, n/a–n/a.

37. Tilton, S. C.; Karin, N. J.; Tolic, A.; Xie, Y.; Lai, X.; Hamilton, R. F.; Waters, K. M.; Holian, A.; Witzmann, F. A.; Orr, G. *Nanotoxicology* **2013**, 1–16.

38. Toh-Boyo, G. M.; Wulff, S. S.; Basile, F. *Analytical Chemistry* **2012**, *84*, 9971–9980.

39. Tsuji, J. S. *Toxicological Sciences* **2005**, *89*, 42–50.

40. Vijayakumar, S.; Ganesan, S. *Journal of Nanomaterials* **2012**, *2012*, 1–9.

41. Yang, X.; Liu, J.; He, H.; Zhou, L.; Gong, C.; Wang, X.; Yang, L.; Yuan, J.; Huang, H.; He, L. *Part Fibre Toxicol* **2010**, *7*, 1.

42. Yang, Z.; Zhang, Y.; Yang, Y.; Sun, L.; Han, D.; Li, H.; Wang, C. *Nanomedicine: Nanotechnology, Biology and Medicine* **2010**, *6*, 427–441.

43. Zhang, X.; Scalf, M.; Berggren, T. W.; Westphall, M. S.; Smith, L. M. *Journal of the American Society for Mass Spectrometry* **2006**, *17*, 490–499.